Probability of Landslide Occurrence Mapping using Probability Density Function in Nam Li Watershed of Thailand

Tanang, S.[1] and Sarapirome, S.[2]
School of Remote Sensing, Institute of Science, Suranaree University of Technology, 111 University Avenue Suranaree, Mueang, Nakhon Ratchasima 30000, Thailand, E-mail: sirilak@g.sut.ac.th[1], sunyas@g.sut.ac.th[2]

Abstract
The study offers local probability density function (PDF) analysis to estimate spatial probability failure index (PFI) which was applied to mapping probability of landslide occurrence of the Nam Li watershed, Uttaradit, Thailand, where big event of landslide occurred in 2007. The PDF analysis required landslide susceptibility indexes (LSIs) as input. They were derived from slope stability model involving ranges of engineering properties and varying slopes of each rock unit. Critical PFI layer of each rock unit was cell-based estimated from one of the candidate LSIs which provided the biggest ratio of landslide scars and PFI equal 1. Critical PFIs of all rock units were divided into 4 classes, namely low, moderate, high, and very high to represent the probability of landslide occurrence of the area in terms of scar-class area ratio as 0.038, 0.051, 0.054, and 0.112, respectively.

1. Introduction

Landslide causes a loss of lives and estate on the earth. Most events occurred in the high slope area with different environment and characteristics that lead to different damage intensity. It can cause a big loss and tragedy if occurs in the densely populated area. In Thailand, the big landslide events were recorded starting from 1970 (DMR, 2011). Many studies were concentrated on mapping landslide susceptibility for land-use and regional planning, and mitigation management (Yumuang, 2006, Jamali and Abdolkhani, 2009, Sartohadi et al., 2010, Intarawichian and Dasananda, 2011 and Cannats et al., 2012). The landslide susceptibility is mapped based on qualitative or quantitative and direct or indirect methods (Guzzetti et al., 1999), and deterministic or non-deterministic (probabilistic) models (Yilmaz, 2010). Referring to Yesilnacar and Topal (2005) and Yilmaz (2010), different size of study areas will dictate suitable input data and analytical processes.

For large area or regional scale, the qualitative methods and probabilistic models are considered more suitable. The susceptible failure can be determined based on the landslide inventory, geologic and geomorphologic characteristics of the potential area. The variety of methods and models for landslide susceptibility studies cover bivariate probability analysis (Bijukchhen et al., 2011 and Yalcin et al., 2011), logistic regression or multivariate analysis (Lee, 2004, Yesilnacar and Topal, 2005, Chen and Wang, 2007, Yilmaz, 2010, Yalcin et al., 2011 and Pourghasemi et al., 2012), fuzzy logic (Pradhan, 2010, Kayastha, 2012, Pourghasemi et al., 2012 and Kayastha et al., 2013), frequency ratio (Lee and Pradhan, 2006, Intarawichian and Dasananda, 2011 and Yalcin et al., 2011), artificial neural network (ANN) (Ermini et al., 2005 and Pradhan and Lee, 2010) and analytical hierarchy process (AHP) (Yoshimatsu and Abe, 2006, Intarawichian and Dasananda, 2010 and Yalcin et al., 2011). The well-known AHP deals with scores and weights of criteria for index calculation, which are more subjective or arbitrary and more likely to depend on the uncertain expert opinions. Most factors used in those models frequently consist of landslide inventory (position and number of scars), geology (lithology, rock unit, and fault line), topographic characteristic (elevation, slope, aspect, and curvature), hydrological (runoff, drainage density, distance to drainage), land use/land cover, road (Yalcin et al., 2011) and other indexes such as topographic wetness index (TWI), stream power index (SPI), and normalized difference vegetation index (NDVI) (Yilmaz, 2010). None of them applies engineering property of materials related to the process of the landslide.

For smaller area or local scale where more spatially detail and accurate result is expected, the geotechnical engineering method which is a quantitative method and physical based model has been selected for landslide susceptibility mapping. The geotechnical engineering method has been widely used during 1998 to present. The slope stability theory based upon infinite slope stability model was used through SINMAP model (Pack et al., 1998 and Zaitchik et al., 2003) and SHALSTAP model (Meisina and Scaravelli, 2007). The SINMAP and SHALSTAP are spatial modelings using GIS technology. The variables include rock/soil properties (cohesion and friction angle) and water condition (Topographic Wetness Index; TWI). These models applied the Factor of Safety (FS) which is a simple slope stability model to assessing landslide probability. Many studies calculated FS using GIS function to indicate landslide probability (Greif et al., 2006 and Omar et al., 2007).

Tanang et al., (2010) applied Factor of Safety (FS) to landslide mapping in term of Landslide Susceptibility Index (LSI) which was calculated from the average properties of rock units. The result showed that high frequency of landslide scars occurred evenly in the whole range of LSIs with no specific pattern (Figure 3). Therefore, it can be concluded that the classification of the potential of landslide occurrence in any area using LSI alone is not possibly valid. This invalid result could be obtained by using average rock properties in LSI estimation in spite of the presence of rock properties of each unit, in fact, existing in range. Due to the spatial complexity of mixed kinds of rocks and their structure in a geological mapping unit, its quantitative engineering properties which relate to landslide always exist in a specific range of number (Wyllie and Mah, 2004, Das, 2007 and Alden, 2010). To cover engineering properties existing in a geological mapping unit as much as possible, the input of them for LSI calculation should be varied to be many values to cover a whole range of properties. Thus, all possible combinations of these properties and slope should be used as representative inputs into the Probability Density Function (PDF), a function which can be used to solve the problem on varying rock properties in slope stability analysis (Wyllie, 1999). Therefore, this research proposes PDF for the probability of landslide occurrence mapping together with slope stability analysis in term of LSI.

2. Study Area

Nam Li Watershed, where big catastrophic landslide event occurred in 2007, is selected to be the study area. It is located in Uttaradit Province, Thailand. The Nam Li watershed is approximately 200 square kilometers. The topography is the mountainous area. Based on geologic map at scale of 1:50,000 (Lamchuan and Sinpunanan, 1987), geology of the area is characterized by rocks ranging in ages from Carboniferous to Triassic and consists of 4 units which are Mae Ta group (Carboniferous phyllitic shale, C), Kiu Lom formation (Permian tuffaceous sandstone, P1), Triassic intrusive igneous rock (biotite granite, gr) and Phra That formation (Triassic red sandstone, Tr1) as displayed in Figure 1.

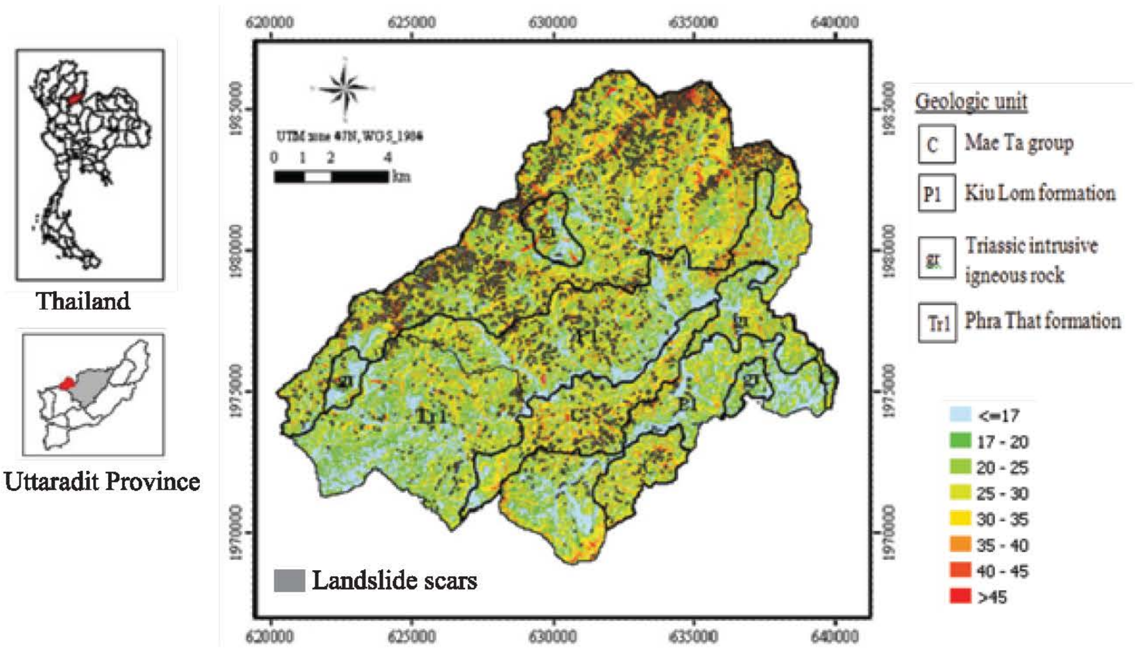

Figure 1: Geology, slope angles of rock-slope polygons, and landslide scars of the event in rock units of Nam Li watershed, Uttaradit, Thailand

The weathering of these rocks covering the whole study area is considered high weathering based on Slake Durability Index (SDI) test which is the method for rock durability determination.

3. Material and Methods

The main methods used in this research consist of slope stability analysis for LSI calculation and probability of failure for PFI determination. There are four steps of the procedure to map Probability of Landslide Occurrence (PLO) as follow 1) data collection and manipulation, 2) LSI analysis, 3) PFI analysis for critical LSI, and 4) PLO mapping as shown in Figure 2.

3.1 Data Collection and Manipulation

The main input data set of LSI analysis consists of engineering properties of rock and slope angle. The properties of each rock unit were collected and analyzed from field investigation and laboratory. Relevant rock properties were assigned as attributes of geologic units which were prepared in form of a GIS vector layer. Boundaries and distribution of geologic units of the study area were based on the geological report and map at a scale of 1:50,000 (Lamchuan and Sinpunanan, 1987 and DMR, 2009) and modified by field investigation data. The attributes of rock properties as input data for slope stability analysis include cohesion, unit weight, and friction angle which are shown in Table 1. Random field samples from the C unit in the study area were tested for cohesion and friction angle by point load strength and direct shear testing. The results are consistent with the properties listed in rock property databases of Goodman (1989), Wyllie and Mah (2004), and Alden (2010). Hence, attributes of rock units were adopted from the databases. From field investigation, landslide scars occurred on weathering rock as a shallow landslide of which thickness is between 1 to 3 meters. Most landslide scars occurred on the shallow surface where weathered rock strata of the units were mixed, indicating by the complicate structure and being heavily fractured due to long time experiencing the tectonic force. This landslide event occurred when pores of material in scars were fully filled by infiltrated water. Thus, the same thicknesses of material (depth of weathered rock above sliding plane) and its saturation when the failure occurred were assigned.

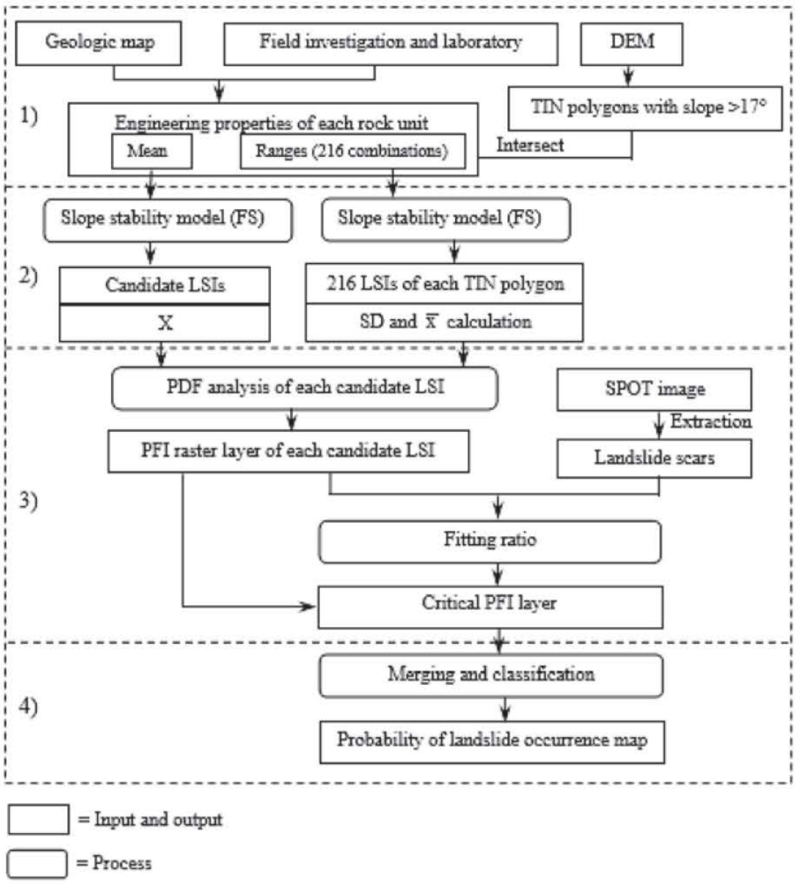

Figure 2: The research procedure

Table 1: Geotechnical properties of rocks of 4 geologic units in the study area

Geologic units	Group/ Formation	Rock Classification	Cohesion, c (kN/m^2)	Unit weight, γ (kN/m^3)	Friction angle, ϕ (degree)
C	Mae Tha	Phyllitic shale	5.0×10^3	23.54×10^3-27.47×10^3	20-27
gr	Intrusive Igneous rock	Biotite granite	55.2×10^3	25.51×10^3-26.49×10^3	34-40
P1	Ratburi/ Kiu Lom	Tuffaceous sandstone	38.4×10^3	21.58×10^3-27.47×10^3	27-34
Tr1	Lampang/ Phra That	Red sandstone	27.2×10^3	23.54×10^3-25.51×10^3	27-34

The mean of each property was calculated for candidate LSIs estimation. To represent all possible properties of each rock unit, engineering properties in ranges were broken down into 6 classes with equal increment. Possible combinations of classes from each property were arranged to represent each rock unit. This resulted in 216 combinations of rock properties for each unit. TIN polygons representing slope faces of the study area were generated from 5 m × 5 m grid DEM of the Land Development Department (LDD), Thailand. The Slope angle of each TIN polygon was estimated by a function in 3D analysis tool of ArcGIS™. However, the slopes of an area that cause material movement on it should not less than 30% or 17.45 degree (Coe et al., 2000 and Mahidol University, 2003).

Then, the TIN polygons with slope ≤17 degree were extracted as insensitive areas. The parameters for LSI calculation were obtained under the domains of geologic units and slope characteristics. Thus, an intersection of TIN slope of sensitive area and rock unit vector layers was performed and resulted in layers of rock-slope polygons which contain attributes of rock properties and slope angles. A layer was represented by a rock unit. For more information, it is better to clarify that the rock-slope polygon layer was derived from layers of TIN and geologic map with difference scales, therefore, the accepted suitable scale of the layer should rely on the scale of a geologic map which is smaller. Sequentially, this suitable scale was transferred to the results of any further analyses.

The landslide scars required for ranking candidate LSIs and estimating fitting ratio were extracted from a SPOT image (Copyright (2006) GISTDA) by visual interpretation.

3.2 LSI Analysis

The LSI analysis of each rock-slope polygon was performed using Factor of Safety (FS), one of the slope stability models. The model variables include rock properties and slope angle. There are many different methods for FS calculation.

Having clear boundaries of landslide scars, the infinite slope stability method was selected for this research. This method is a 1D model which is most commonly employed for the purpose (Mergili and Fellin, 2009 and Das, 2007). The FS is the ratio between resisting and driving forces. The resisting force is the shear strength (τ_r) and the driving force is the shear stress (τ_d). The equations involve the Mohr-Coulomb failure criterion as shown in Equation 1 and Equation 2:

$$FS=\frac{\tau_r}{\tau_d}$$

Equation 1

When the force acts on slope plane with β (degree) slope angle, the FS can be calculated by:

$$FS=\frac{c+\left(\gamma\cdot Z-\gamma_w\cdot Z_w\right)\cdot\cos^2\beta\cdot\tan\phi}{\gamma\cdot Z\cdot\sin\beta\cdot\cos\beta}$$

Equation 2

Where c is the cohesion (kN/m^2), γ is the unit weight of material (kN/m^3), γ_w is the unit weight of water (9.81 kN/m^3), Z is the thickness of slope material above sliding plane (m), Z_w is the thickness of saturated slope material above sliding plane (m), and ϕ is the internal friction angle (degree).

According to several previous studies (Wyllie, 1999, U.S. Army Corps of Engineers, 2003; Wyllie and Mah, 2004, Das, 2007, Cheng and Lau, 2008 and Mergili and Fellin, 2009), the slope failure will occur when the driving force is bigger than the resistance force. This statement is more likely to apply properly to site investigation, not for the area of the geologic rock unit. The FS values or called LSIs in this study, calculated from Equation 2, relatively indicate where slope failure could occur in the geologic rock unit. The LSIs of rock-slope polygons were then derived using their mean and 216 combinations of rock properties. The rock-slope polygons layers of 4 rock units with LSIs derived from the ***mean*** properties were converted to be raster layers with 5 m × 5 m cell size, corresponding to original grid DEM data used. Then, LSIs from cells and cells of landslide scars were plotted against their frequencies. The ranges of candidate LSIs of rock units were then obtained by matching to the distribution ranges of the scars. From ***216 combinations*** of each rock-slope polygon, 216 LSIs were derived. Then, mean and SD of them from each polygon were calculated for further PFI analysis.

3.3 PFI Analysis

As above mentioned, there were many candidate LSIs of each rock unit. Additionally, when dealing with the uncertainty of engineering properties of rock units which appear in ranges, the variation of LSIs would occur to represent all possible combinations of properties. To overcome this, LSIs of each TIN polygon of any rock unit should be better transformed to be the PFI by the use of PDF (Wyllie, 1999). PFI analysis was therefore applied to choose a critical PFI layer from the candidates. Critical PFI layer expressed areas having probability of landslide occurrence more accurately.

The analysis includes PFI calculation using the PDF and the selection of the best PFI which provides the highest spatial fitting ratio between cells of PFI equal 1 and scar cells. Cells containing PFI equal 1 indicate 100% of landslide occurrence probability. PDF performs the rock-slope-polygon-based calculation using normal distributing LSIs and their mean and SD, which can be defined as (Wyllie, 1999):

$$f(x) = \frac{1}{SD\sqrt{2\pi}} \exp\left[-\frac{1}{2}\left(\frac{x_i - \overline{x}}{SD}\right)^2\right]$$

Equation 3

Where x_i is a set of LSIs, i = 1,..., n, n = 216, $\overline{x}$ is the mean of LSIs, SD is the standard deviation of LSIs. The PDF calculation of each rock-slope polygon resulted in the probability distribution of 216 LSIs. Theoretically, these probabilities were plotted against 216 LSIs. Then, each candidate LSI was applied to identifying the probability of failure of each plot. The candidate LSI value separates area under the curve to be negative and positive zone. The area under the curve in the negative portion zone can be calculated to be the PFI. The PFI range is between 0-1. This performance was operated by the specific function of Microsoft® Excel. However, the candidate LSI which provides PFI equal 1 to more polygons might not be the critical LSI for that rock unit. But the one that provides polygons with PFI equal 1 matching more to landslide scars is. Therefore, the fitting ratio to determine the matching area was required. The layers of rock-slope polygons containing PFIs achieved from all candidate LSIs were converted to be candidate PFI raster layers (5 m × 5 m resolution) for matching.

Fitting Ratio (FR) was designed to select a critical PFI layer from the candidates. The ratio represents the proportion of the intersection ($A \cap B$) and union ($A \cup B$) of scar cells (A) and cells of PFI equal 1 (B). The ratio can be expressed as:

$$FR = \frac{(A \cap B)}{(A \cup B)}$$

Equation 4

The candidate PFI layer provided the highest ratio was identified as the critical PFI layer.

3.4 Spatial Distribution Comparison of Probability of Landslide Occurrence and Scars

The critical PFI layer of the study area was obtained from the merging of 4 critical PFI layers of rock units. For the display purpose, the layer was classified to be 4 classes by equal range, reflecting the distribution of probability of landslide occurrence. The consistency of the probability and actual occurrence was observed when compared the frequencies of each class and landslide scars in the same class.

4. Result and Discussion

According to the methods described above, the results are as follows:

4.1 Rock Properties and Slope Angles of Rock Units

From 6 classes of each engineering property, 216 combinations of each rock unit were formed up. Table 2 shows parameters of classes and their means. The slope angles generated from TIN polygons fall into the range of 0.22-53.52 degree. TIN polygons with slope angle >17 degree were extracted to be sensitive areas. The intersection of these sensitive polygons and geology resulted in rock-slope polygons. The slope angles of polygons were classified into 8 classes to display their spatial distribution together with landslide scars of the event in rock units (Figure 1). It confirms that all landslide scars existed in the area falling into polygons with slope angle > 17 degree.

Table 2: The parameters of classes and their means for LSI calculation

Class	C unit (c = 5.0×10^3 kN/m^2)					P1 unit (c = 38.4×10^3 kN/m^2)		
	γ□(kN/m^3)	ϕ□(degree)	Z (m)	Z_w (m) (m)	γ (kN/m^3)	ϕ□(degree)	Z (m)	Z_w (m)
1	23540	13.0	1.0	1.0	21580	27.0	1.00	1.00
2	23804	14.0	1.4	1.4	22758	28.4	1.40	1.40
3	24068	15.0	1.8	1.8	23936	29.8	1.80	1.80
4	24332	16.0	2.2	2.2	25114	31.2	2.20	2.20
5	24596	17.0	2.6	2.6	26292	32.6	2.60	2.60
6	24860	18.0	3.0	3.0	27470	34.0	3.00	3.00
Mean	21200	15.5	2.0	2.0	24525	30.5	2.0	2.0
Class	gr unit (c = 55.2×10^3 kN/m^2)					Tr1 unit (c = 27.2×10^3 kN/m^2)		
	γ□(kN/m^3)	ϕ□(degree)	Z (m)	Z (m)	γ□(kN/m^3)	ϕ□ (degree)	Z (m)	Z_w (m)
1	25510	34.0	1.00	1.00	23540	27.0	1.00	1.00
2	25706	35.2	1.40	1.40	23934	28.4	1.40	1.40
3	25902	36.4	1.80	1.80	24328	29.8	1.80	1.80
4	26098	37.6	2.20	2.20	24722	31.2	2.20	2.20
5	26294	38.8	2.60	2.60	25116	32.6	2.60	2.60
6	26490	40.0	3.00	3.00	25510	34.0	3.00	3.00
Mean	26000	37.0	2.0	2.0	24525	30.5	2.0	2.0

Table 3: The candidate LSIs of rock units

Geologic units	LSIs ranges	Candidate LSIs
C	0.630-1.603	0.63, 0.70, 0.80, 0.90, 1.00, 1.10, 1.20, 1.30, 1.40, 1.50, 1.60, and 1.603
gr	1.026-3.196	1.026, 1.10, 1.20, 1.30, 1.40, 1.50, 1.60, 1.70, 1.80, 1.90, 2.00, 2.10, 2.20, 2.30, 2.40, 2.50, 2.60, 2.70, 2.80, 2.90, 3.00, 3.10, and 3.196
P1	0.926-2.480	0.926, 1.00, 1.10, 1.20, 1.30, 1.40, 1.50, 1.60, 1.70, 1.80 1.90, 2.00, 2.10, 2.20, 2.30, 2.40, and 2.480
Tr1	0.768-2.317	0.768, 0.80, 0.90, 1.00, 1.10, 1.20, 1.30, 1.40, 1.50, 1.60, 1.70, 1.80, 1.90, 2.00, 2.10, 2.20, 2.30, and 2.317

Table 4: Some examples of mean and SD of 216 LSIs from TIN polygons

Polygon ID	1	2	3	...	214	215	216	Mean	SD
0	1.90609	1.98950	2.07516	...	2.04706	2.13780	2.23142	2.34758	1.78988
1	1.75111	1.82719	1.90531	...	1.79661	1.87696	1.95971	2.15377	1.64240
2	2.17228	2.26813	2.36655	...	2.23688	2.33811	2.44237	2.67958	2.04259
3	1.47528	1.53818	1.60275	...	1.50696	1.57338	1.64179	1.80815	1.37948
.	.	.	.		.	.	.	.	.
.	.	.	.	...	.	.	.	.	.
.	.	.	.		.	.	.	.	.
9646	1.35025	1.40706	1.46538	...	1.37503	1.43502	1.49680	1.65088	1.25990
9647	1.24237	1.29380	1.34660	...	1.26055	1.31486	1.37080	1.51456	1.15631
9648	1.29569	1.34977	1.40529	...	1.31710	1.37420	1.43303	1.58190	1.20748

4.2 Resulting LSIs

The LSI analysis using mean rock properties of rock-slope polygons in the sensitive area resulted in various LSIs. They were converted to be LSIs raster layer. Then, frequencies of scar cells and sensitive cells were plotted according to varying LSIs to show the relationship between their spatial distributions in each rock unit (Figure 3). From the plot of each rock unit, the observable frequencies of both appear to be in the same ranges of LSIs. It is observable that the high frequencies of scar cells are more likely associated with low LSIs of each rock unit. This reflects that the scars occurred more in low resistant zone of rock units.

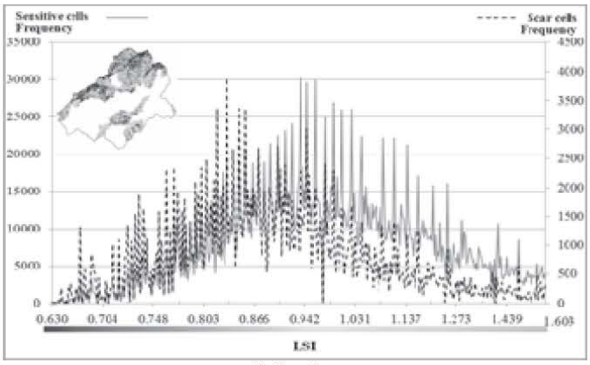

a) C unit

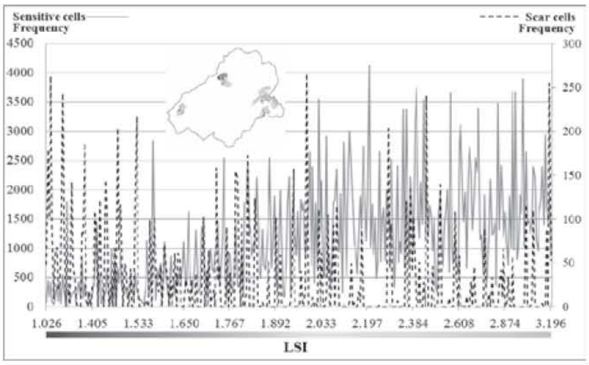

b) gr unit

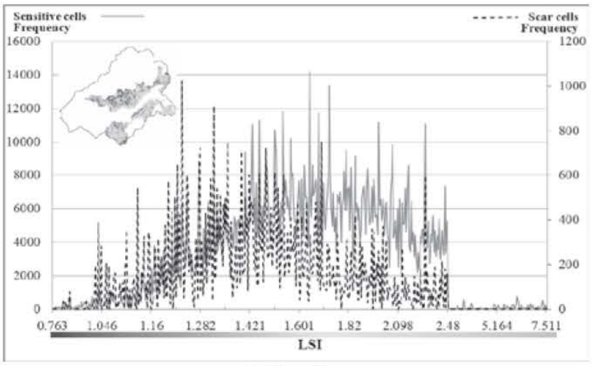

c) P1 unit

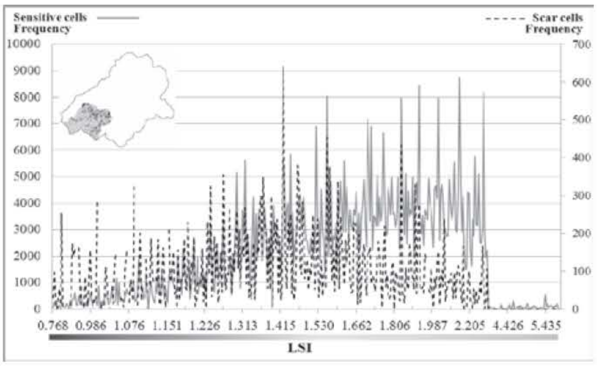

d) Tr1 unit

Figure 3: The relation of sensitive and scar areas frequency and LSIs

Therefore, the range of candidate LSIs of each rock unit can be determined and broken down with 0.10 increments as shown in Table 3. These LSIs become candidates of a critical LSI finding. It means that one of them can be the most sensitive LSI indicating the highest probability of landslide occurrences in a rock unit area. Table 4 shows examples of 216 LSIs of each rock-slope polygon calculated from combinations of rock properties in ranges. Their mean and SD were also calculated for further input to PFI analysis.

4.3 Critical PFI Layer

The PFIs of all TIN polygons of each rock unit were calculated under each candidate LSI and transformed to be raster layers as shown in Figure 4. The cells with PFI equal 1 are depicted in red while the ones with PFI less than 1 are in green. The scar cells are depicted in black.

Obviously, the number of red cells and their association with the scar cells are increased with increasing candidate LSI. In contrast, the number of green cells and their association with the scar cells are increased with decreasing LSI as well. Therefore, the FR of each candidate PFI raster layer was calculated and the results are shown in Figure 4. From the results, critical PFI layers of C, gr, P1, and Tr1 units were achieved from the critical LSI of 1.2, 1.8, 1.7, and 1.6 and their best fitting ratios are 0.143, 0.159, 0.082, and 0.095, respectively.

4.4 Probability of Landslide Occurrence

The merged critical PFI layer or the map of probability of landslide occurrence (PLO map) was then classified into 4 classes namely, low, moderate, high, and very high, using equal ranging as shown in Figure 5. The ratios between scar cells and cells of classes of the study area and each rock unit were estimated and shown in Figure 6. The result shows that the higher probability class is associated with the higher ratio as obviously expressed in the plot of the whole study area. Nevertheless, the ratios of moderate and high classes of C and Tr1 units are almost the same. The reason to explain this is the areas of these 2 classes of these rock units are comparatively very small compared to their low and very high classes. The higher ratio in high and very high classes indicates the more sensitive rock unit to landslide occurrence. The C unit shows highest sensitive, follow by gr, Tr1, and P units, respectively. It is interesting to note that the high and very high classes of gr unit express suddenly high ratio or more sensitive compared to other units.

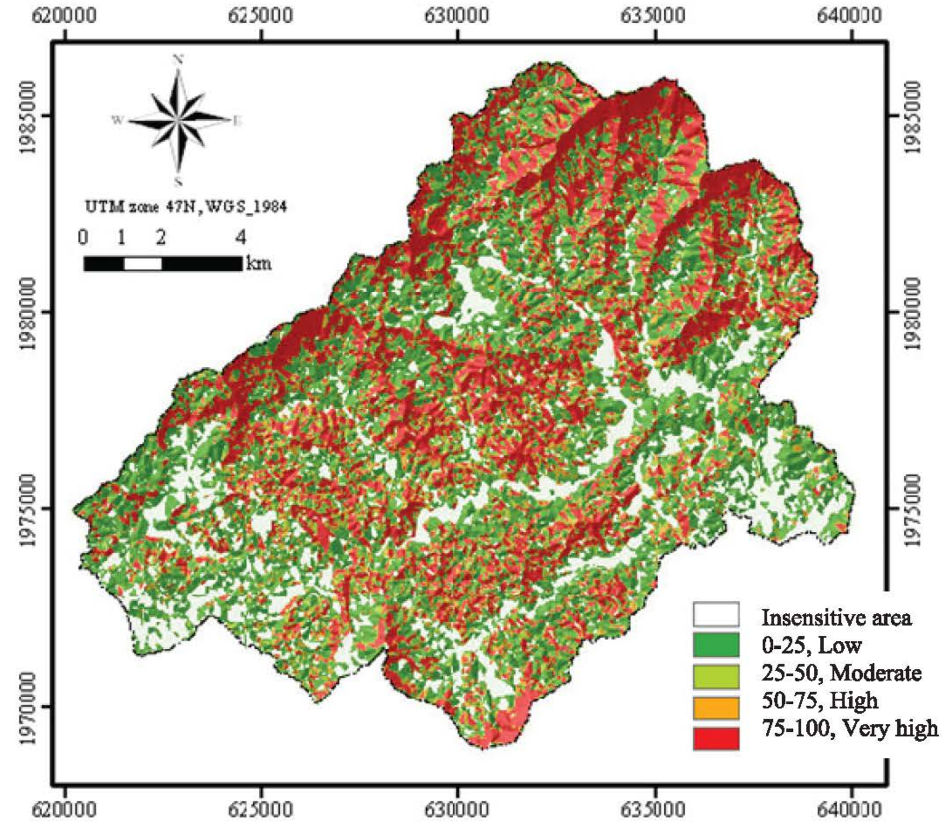

Figure 5: Probability of landslide occurrence map

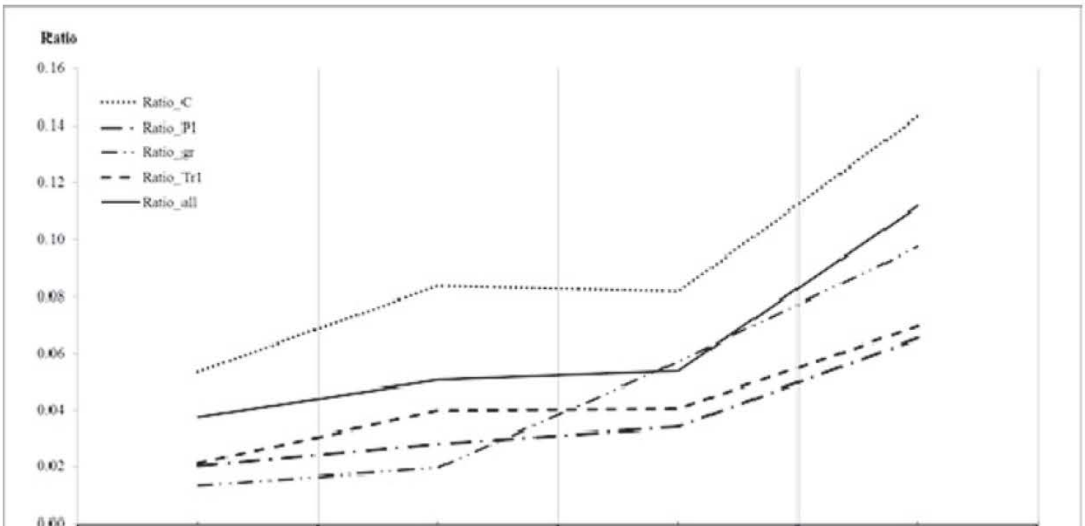

	Low PFI = 0-25			Moderate PFI = 26-50			High PFI = 51-75			Very high PFI = 76-100		
	Ratio	Area	Scars	Ratio	Area	Scars	Ratio	Area	Scars	Ratio	Area	Scars
C	0.054	1,504,101	80,514	0.084	130,085	10,912	0.082	121,365	9,933	0.143	1,555,621	222,886
P1	0.020	586,918	11,941	0.028	131,702	3,727	0.034	132,123	4,521	0.065	764,201	50,052
gr	0.014	302,176	4,142	0.020	20,451	404	0.057	11,035	630	0.098	53,166	5,186
Tr1	0.021	404,906	8,565	0.040	72,508	2,883	0.041	63,782	2,594	0.070	304,590	21,218
All	0.038	2798101	105162	0.051	354746	17926	0.054	328305	17678	0.112	2677578	299342

Figure 6: The ratios between scar cells and cells of classes of the study area

5. Conclusion

The study result reveals that utilization of PDF for PLO mapping can provide more valid result than applying LSI alone. The scar-class area ratios of PLO classes show the positively linear relationship with PFI while no such relationship appeared when LSI alone was directly applied. The spatial relationship of landslide scars and LSI is random. This confirms that PDF operating on LSIs derived from existing ranges of rock properties expressed more relationship to the scars than LSIs derived from merely the mean rock properties. Particularly, when the rock properties in ranges of each unit were input in the process to obtain local PFI layer derived from critical LSI of the unit. These local PFI layers can provide the spatial distribution of probability of landslide occurrence better than global PFI layer derived from properties representing the whole study area. Theoretically, critical LSIs of certain rock units should be applicable in potential landslide mapping of any other areas characterized by the same rock units. This concept can be assured when the results from the same approach of other events and study areas are consistent with results from this study. Basically, the findings of the study could be useful for the risk assessment and mitigation measure to reduce the risk of the landslide prone areas in general, wherever people and their activities are involved.

Reference

Alden, A., 2010, *Density of Common Rock Type,* http://geology.about.com/cs/rock_types/a/aarockspecgrav.htm.

Bijukchhen, S. M., Kayastha, P. and Dhital, M. R., 2011, A Comparative Evaluation of Heuristic and Bivariate Statistical Modeling for Landslide Susceptibility Mappings in Ghurmi-Dhad Khola, East Nepal. *Arabian Journal of Geosciences*, 6, 2727-2743.

Cannats, M., Molinarl, M. E., Xuan Luan, T. and Hung Long, N., 2012, Web Processing Services for Shallow Landslide. *International Journal of Geoinformatics*, 8(1), 25-34.

Cheng, Y. M. and Lau, C. K., 2008, *Slope Stability Analysis and Stabilization*, (New York: Routledge).

Chen, Z. and Wang, J., 2007, Landslide Hazard Mapping using Logistic Regression Model in Mackenzie Valley, Canada. *Natural Hazard*, 42(1), 75-89.

Coe, J. A., Michael, J. A., Crovelli, R. A. and Savage, W. Z., 2000, *Preliminary Map Showing Landslide Densities, Mean Recurrence Intervals and Exceedance Probabilities as Determined from Historic Records*. Seattle, Washington. Open-file report 00-303, U.S. Geological Survey.

Das, B. M., 2007, *Principles of Geotechnical Engineering*, (Toronto: Nelson).

DMR, 2009, *Geological Map of Thailand 1:50,000*. Cartographic Section, Department of Mineral Resource, Ministry of Natural Resources and Environment All rights reserved, Thailand.

DMR, 2011, Landslide record. http://www.dmr.go.th/main.php?filename=landslide_record.

Ermini, L., Catani, F. and Casagli, N., 2005, Artificial Neural Networks Applied to Landslide Susceptibility Assessment. *Geomorphology*, 66(1), 327-343.

Greif, V., Sassa, K. and Fukuoka, H., 2006, Failure Mechanism in an Extremely Slow Rock Slide at Bitchu-Matsuyama Castle Site (Japan). *Landslides*, 3(1), 22-38.

Guzzetti, F., Carrara, A., Cardinali, M. and Reichenbach, P., 1999, Landslide Hazard Evaluation: A Review of Current Techniques and their Application in a Multi-Scale Study, Central Italy. *Geomorphology*, 31, 181-216.

Goodman, R. E., 1989, *Introduction to Rock Machanics*. (New York: John Wiley & Sons).

Intarawichian, N. and Dasananda, S., 2010, Analytical Hierarchy Process for Landslide Susceptibility Mapping in Lower Mae Chaem Watershed, Northern Thailand. *Suranaree Journal of Science and Technology*, 17(3), 277-292.

Intarawichian, N. and Dasananda, S., 2011, Frequency Ratio Model Based Landslide Susceptibility Mapping in Lower Mae Chaem watershed, Northern Thailand. *Environmental Earth Sciences*. 64(8), 2271-2285.

Jamali, A. A. and Abdolkhani, A., 2009, Preparedness against Landslide Disasters with Mapping of Landslide Potential by GIS- SMCE (Yazd-Iran). *International Journal of Geoinformatics*, 5(4), 25-31.

Kayastha, P., 2012, Application of Fuzzy Logic Approach for Landslide Susceptibility Mapping in Garuwa Sub-Basin, East Nepal. *Journal of Environment and Earth Science*, 6(4), 420-432.

Kayastha, P., Bijukchhen, S. M., Dhital, M. R. and Smedt, F. D., 2013, GIS Based Landslide Susceptibility Mapping using a Fuzzy Logic Approach: A Case Study from Ghurmi-Dhad Khola Area, Eastern Nepal. *Journal Geological Society of India*, 82, 249-261.

Lamchuan, A. and Sinpunanan, S., 1987. *Geology of Sirikiti Dam Sheet and Amphor Tha Pla Sheet*. Department of Mineral Resources, Thailand.

Lee, S., 2004, Application of Likelihood Ratio and Logistic Regression Models to Landslide Susceptibility Mapping using GIS. *Environmental Management*. 34(2), 223-232.

Lee, S. and Pradhan, B., 2006, Landslide Hazard Mapping at Selangor, Malaysia using Frequency Ratio and Logistic Regression Models. *Landslides*, 4(9), 33-41.

Mahidol University, 2003, *The Study Of Landslide Risk Area (final report)*, Engineering Data and Research Center, Faculty of Engineering, Mahidol University, Thailand.

Meisina, C. and Scarabelli, S., 2007, A Comparative Analysis of Terrain Stability Models for Predicting Shallow Landslides in Colluvial Soils. *Geomorphology*, 87, 207-223.

Mergili, M. and Fellin, W., 2009, Slope Stability and Geographic Information Systems: An Advanced Model Versus the Infinite Slope Stability Approach. *In Russian Academy of Sciences, Problems of Decrease in Natural Hazards and Risks, The International Scientifically-Practical Conference GEORISK 2009*, 119-124.

Omar, H., Ibrahim, A. L. and Hashim, M., 2007, Slope Stability Analysis using Remote Sensing Data. *Paper Presented at the 28th Asian conference on Remote Sensing (ACRS 2007)*, Putra World Trade Center, Kuala Lumpur, Malaysia.

Pack, R. T., Tarboton, D. G. and Goodwin, C. N., 1998, SINMAP a Stability Index Approach to Terrain Stability Hazard Mapping. *SINMAP User's Manual*. Terratech Consulting Ltd, Salmon Arm, B.C., Canada.

Pradhan, B. and Lee, S., 2010, Delineation of Landslide Hazard Areas on Penang Island, Malaysia, by using frequency Ratio, Logistic Regression and Artificial Neural Network Models. *Environmental Earth Sciences*, 60: 1037-1054.

Pourghasemi, H. R., Mohammady, M. and Pradhan, B., 2012, Landslide Susceptibility Mapping using Index of Entropy and Conditional Probability Models in GIS: SafaroodBasin, Iran. *Catena*, 97, 71-84.

Pourghasemi, H. R., Pradhan, B. and Gokceoglu, C., 2012, Application of Fuzzy Logic and Analytical Hierarchy Process (AHP) to Landslide Susceptibility Mapping at Haraz Watershed, Iran. *Natural Hazards*, 63(2), 965-996

Pradhan, B., 2010, Application of an Advanced Fuzzy Logic Model for Landslide Susceptibility Analysis. *International Journal of Computational Intelligence Systems*, 3(3), 370-381.

Sartohadi, J., Samodra, G. and Sri Hadmoko, D., 2010, Landslide Susceptibility Assessment using Heuristic Statistically Method in Kayangan Catchment Kulon Progo Yogyakarta-Indonesia. *International Journal of Geoinformatics*, 6(3), 23-28.

Tanang, S., Sarapirome, S. and Pliklang, S., 2010, Landslide Susceptibility Map of Nam Li Watershed, Uttaradit, Thailand. *Proceedings of the 31th Asian Conference on Remote Sensing 2010*, Nov 01-05, Hanoi, Vietnam.

U.S. Army Corps of Engineers, 2003, Engineering and Design: Slope Stability. *Engineer Manual*. Department of the Army, U.S. Army Corps of Engineers, Washington, DC.

Wyllie, D. C., 1999, *Foundations on Rock*. 2nd edition. (London: E & FN Spon).

Wyllie, D. C. and Mah, C. W., 2004, *Rock Slope Engineering: Civil and Mining*, 4th edition. (New York: Spon Press).

Yalcin, A., Reis, S., Aydinoglu, A. C. and Yomralioglu, T., 2011, A GIS-Based Comparative Study of Frequency Ratio, Analytical Hierarchy Process, Bivariate Statistics and Logistics Regression Methods for Landslide Susceptibility Mapping in Trabzon, NE Turkey. *Catena*, 85, 274-287.

Yesilnacar, E. and Topal, T., 2005. Landslide Susceptibility Mapping: A Comparison of Logistic Regression and Neural Networks Methods in A Medium Scale Study, Hendek Region (Turkey), *Engineering Geology*, 79, 251-266.

Yilmaz, I., 2010. Comparison of Landslide Susceptibility Mapping Methodologies for Koyulhisar, Turkey: Conditional Probability, Logistic Regression, Artificial Neural Networks, and Support Vector Machine. *Environmental Earth Sciences*, 61, 821-836.

Yoshimatsu, H. and Abe, S., 2006, A Review of Landslide Hazards in Japan and Assessment of their Susceptibility using an Analytical Hierarchic Process (AHP) Method. *Landslides*, 3, 149-158.

Yumuang, S., 2006, 2001 Debris Flow and Debris Flood in Nam Ko Area, Phetchabun Province, Central Thailand. *Environmental Geology*, 51, 545-564.

Zaitchik, B. F., Van Es, H. M. and Sullivan, P. J., 2003, Modeling Slope-Stability in Honduras: Parameter Sensitivity and Scale of Aggregation. *Soil Science Society of America Journal*. 67, 268-278.